J. Cent. South Univ. (2015) 22: 2533−2539
DOI: 10.1007/s11771-015-2782-5

Springer

Crack spacing threshold of double cracks propagation for large-module rack

ZHAO Tie-zhu(赵铁柱), SHI Duan-wei(石端伟), YAO Zhe-hao(姚哲皓),
MAO Hong-yong(毛宏勇), CHENG Shu-xiao(程术潇), PENG Hui(彭惠)

School of Power and Mechanical Engineering, Wuhan University, Wuhan 430072, China

Abstract: Large-module rack of the Three Gorges shiplift is manufactured by casting and machining, which is unable to avoid slag inclusions and surface cracks. To ensure its safety in the future service, studying on crack propagation rule and the residual life estimation method of large-module rack is of great significance. The possible crack distribution forms of the rack in the Three Gorges shiplift were studied. By applying moving load on the model in FRANC3D and ANSYS, quantitative analyses of interference effects on double cracks in both collinear and offset conditions were conducted. The variation rule of the stress intensity factor (SIF) influence factor, R_K, of double collinear cracks changing with crack spacing ratio, R_S, was researched. The horizontal and vertical crack spacing threshold of double cracks within the design life of the shiplift were obtained, which are 24 and 4 times as large as half of initial crack length, c_0, respectively. The crack growth rates along the length and depth directions in the process of coalescence on double collinear cracks were also studied.

Key words: large-module rack; double cracks; fatigue crack propagation; crack spacing threshold; moving load

1 Introduction

The module of the rack in the Three Gorges gear/rack climbing shiplift is 62.67 mm, manufactured by casting and machining method. The inspection report of the finished rack shows that the teeth contain slag inclusions and surface cracks which are in group style. The length and depth of the cracks are 3−10 mm and 3−9 mm, respectively. In order to ensure the safety operation of the Three Gorges shiplift gear/rack within its design life (70 years), it is essential to study the crack propagation rule and the residual life estimation method of large-module rack.

In recent years, the 3D fatigue crack growth rate, trajectories and residual life of single crack in medium and small module gear were studied [1−4]. On the other hand, studies on multiple crack propagation were mainly focused on the theoretical exploration. The interference effects on stress intensity factors of double collinear cracks on a finite flat plate model were studied [5]. Based on the maximum crack opening displacement, computing method of stress intensity factor of double-collinear-through crack tips in the semi-infinite flat plate model was determined [6−7].

Based on a semi-infinite solid model, factors influencing the double parallel offset corrosion crack propagation were studied, and it was revealed that the relative position of cracks is the primary factor [8−10]. S-FEM method was used to study the coalescing process of collinear double cracks of nuclear structure [11] and TAN and CHEN [12] proposed a quantitative prediction method aiming at forecasting short cracks coalescing process. However, the research achievements of the gear/rack crack propagation involved in the large-module as well as the initial cracks and inclusions have not been found.

By applying moving load on the model in FRANC3D and ANSYS, and studying the possible crack distribution forms on Three Gorges shiplift rack, the interference effects on double cracks in both collinear and offset conditions were analyzed quantitatively. The influence factor, R_K, of SIF of double collinear cracks changing with crack spacing ratio, R_S, and the vertical and horizontal crack spacing threshold of double cracks within the design life of the shiplift were obtained. The crack growth rates along the length and depth directions in the process of coalescence on double collinear cracks were also studied. The research achievements can be applied in the life prediction of gear/rack in the Three Gorges shiplift, the Xiangjiaba shiplift and gear transmission of major equipment.

Foundation item: Project(0722018) supported by the China Three Gorges Corporation; Project(2012KJX01) supported by the Hubei Key Laboratory of Hydroelectric Machinery Design & Maintenance, China
Received date: 2014−07−01; **Accepted date:** 2014−11−10
Corresponding author: SHI Duan-wei, Professor, PhD; Tel: +86−27−68774383; E-mail: dwshi@whu.edu.cn

2 Loading method and simulation model

2.1 Moving load

The load on a tooth of the rack is a moving load of which the magnitude and location change over time. In the research of fatigue crack propagation of the rack, the highest point of single tooth contact method and tooth top loading method [1, 13] are widely adopted. For precisely simulating the load case of gear/rack in working conditions, in this work, a moving load method is introduced. Each tooth surface of the rack is discretized into 15 loading regions which contain 6 double teeth-meshing regions, 3 single teeth-meshing regions and 6 double teeth-meshing regions arranging from the top of the tooth to the root of the tooth successively. When the Three Gorge shiplift is under the condition of +10 cm water depth error, the tangential force F_X=1048 kN and radial force F_Y=381 kN are obtained. They are applied on single teeth-meshing area of the rack. According to the gear meshing principle (Fig. 1), the load of 15 loading regions of the rack can be computed by

$$\begin{cases} F_{Xi}=[d_0+b_0(\dfrac{i}{6})]\times F_X,\ i=1,2,3,4,5,6 \\ F_{Xi}=F_X,\ i=7,8,9 \\ F_{Xi}=[(d_0+b_0)-b_0\times\dfrac{(i-10)}{6}]\times F_X, \\ \quad i=10,11,12,13,14,15 \\ F_{Yi}=F_{Xi}\times\tan 20° \end{cases} \tag{1}$$

where d_0=0.4 and b_0=0.2.

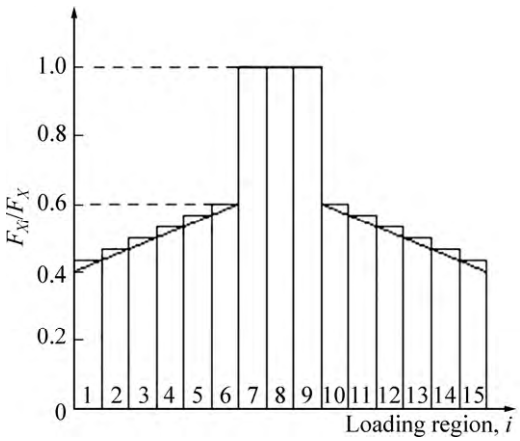

Fig. 1 Loading method of moving load

2.2 Crack propagation and simulation model

Based on the linear elastic fracture mechanics theory, the main control parameter of fatigue crack growth rate is the stress intensity factor amplitude, ΔK, of the crack front points. In terms of the stable propagation region of the crack, the fatigue crack growth rate, da/dN, is computed by Paris' model. The rate is given by

$$\frac{\mathrm{d}a}{\mathrm{d}N}=C(\Delta K)^m \tag{2}$$

where C and m are the material properties. Considering the complexity and the diseconomy of experiments of fatigue crack growth rate, C and m are obtained by the finite element numerical simulation method [14]. Compared with the steel fatigue subcritical crack propagation rate in Ref. [15], the accuracy and the reliability of the finite element method can be verified. The material of the rack is G35CrNiMo6-6+QT1 of which C and m are taken to be 9.412×10^{-12} (mm/r)/(MPa·mm$^{0.5}$)^m and 2.85, respectively.

The fatigue life is the load cycle number, N_C, during which the initial crack depth, a_0, grows to critical crack depth, a_c. The expression of crack fatigue life, N_C, is

$$\begin{cases} N_C=\dfrac{1}{C(f\Delta\sigma\sqrt{\pi})^m(0.5m-1)}\left(\dfrac{1}{a_0^{0.5m-1}}-\dfrac{1}{a_c^{0.5m-1}}\right), \\ \quad m\neq 2 \\ N_C=\dfrac{1}{C(f\Delta\sigma\sqrt{\pi})^m}\mathrm{In}\left(\dfrac{a_c}{a_0}\right),\ m=2 \end{cases} \tag{3}$$

where f is the geometric correction factor; $\Delta\sigma$ is the maximum cyclic stress. In terms of large-module rack, technical requirements demand that the rack must be detected by ultrasonic examination and magnetic particle examination. The acceptance complies with DIN EN 1369, DIN 1690-2 and other relevant standards in which crack length, 2c, is the standard judge parameter. Comprehensively considering the acceptance standards and the crack detection methods during the design life of the rack, the crack length, 2c, corresponding to crack depth, a, under the same load cycle number, N, is considered as the standard judge parameter.

The fatigue crack propagation analysis processes in FRANC3D are as follows:

1) Use ANSYS pre-processing tools to create a crack-free mesh rack. Due to the large size of the rack, the mesh model is divided into crack propagation sub-model, LOCAL (containing the initial crack) and external constraint model, GLOBLE (containing the load and constraints) (Fig. 2).

2) Define moving load in ANSYS pre-processing program by dividing the tooth surface of the rack into 15 loading regions and write load step files LOAD CASE1−LOAD CASE15.

3) Import LOCAL to FRANC3D, insert initial double cracks and remesh the sub-model.

4) Import the external constraint model, GLOBAL, and 15 load step files, and then coalesce the sub-model,

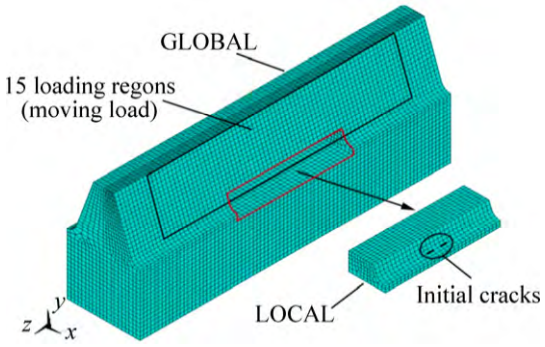

Fig. 2 Simulation model of large-module rack

LOCAL, which contains the initial double cracks and the external constraint model, and GLOBAL, which contains the constraint.

5) Compute the sub-model with initial double cracks by ANSYS automatically.

6) Read the stress analysis results, compute stress intensity factor of the front points of the cracks, analyze crack propagation, update crack front position and remesh the sub-model in FRANC3D.

7) Repeat steps 4)−6), until the end of the fatigue crack propagation.

3 Horizontal spacing threshold of double collinear cracks

3.1 Crack propagation before process of coalescence

In order to describe interference effects between double collinear cracks on large-module rack quantitatively, and further, to explore their horizontal crack spacing threshold, double semi-elliptical collinear cracks in the same size are suggested to insert in the root of the rack tooth on the sub-model. According to the nondestructive testing on the rack of Three Gorges shiplift, the initial crack sizes are set as follows: depth a_0=3 mm, and length $2c_0$=6 mm.

Aiming at searching the horizontal crack spacing threshold on collinear cracks, the golden search method is used. And then, interference effects between collinear cracks are described quantitatively. Double collinear cracks propagation models in the cases of the horizontal spacing S=$2c_0$, $8c_0$, $14c_0$, $18c_0$, $24c_0$ are simulated. Based on the interference effects, mutual strengthening effect exists in crack tips during the propagation process of double collinear cracks. The stress intensity factor, K_I, reflects the interference degree. Aiming at evaluating the strengthening effect of inner and outer crack tips (B and D), the stress intensity factor of single crack tips is defined as K_{I_single} and the influence factor of stress intensity factor R_K=$K_{I(B,D)}$/ K_{I_single} is introduced.

After calculating the R_K and R_S, respectively, in the cases of the horizontal spacing S=$8c_0$, $14c_0$, $18c_0$, $24c_0$, the variation rule of the R_K changing with R_S is obtained. Figure 3 shows that the strengthening effect of inner crack tips (B and C) is much greater than that of outer crack tips (A and D). The curves in Fig. 3(a) almost share the same rule, which indicates that, basically, the change of R_K has nothing to do with S, but is only related to R_S. Through making nonlinear curve fitting by the least squares method, the function relationship between R_K of inner crack tips and R_S is obtained. The function relationship is given by

$$R_K = 0.01136 \times R_S^{-1.021} + 0.9981 \quad (4)$$

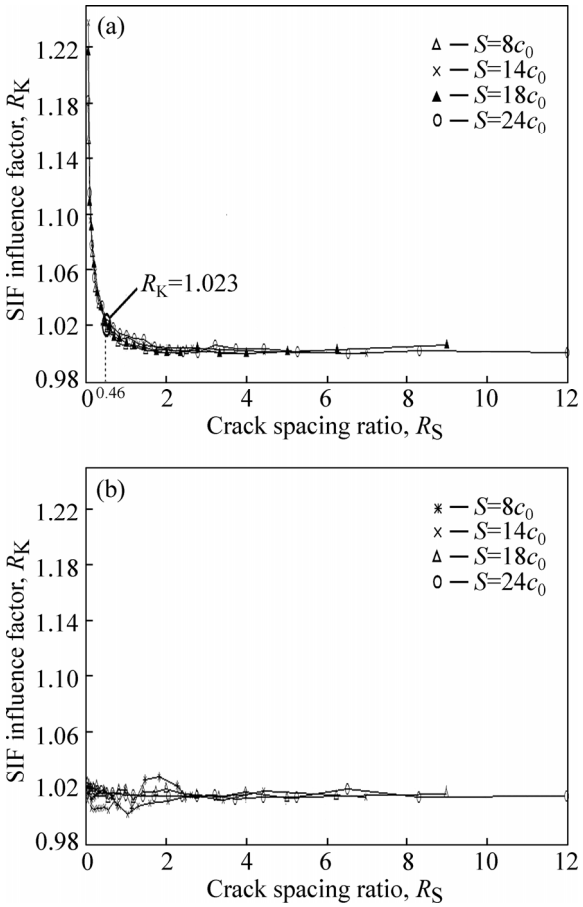

Fig. 3 Relationship between influence factor of SIF and crack spacing ratio under various horizontal spacings: (a) Inner crack tips; (b) Outer crack tips

The relationship between R_K and R_S of inner crack tips is shown in Fig. 3(a) and Eq. (4). When R_S>1, R_K<1.01 and R_K≈1. Then, there are no interference effects between double collinear cracks and the two cracks are isolated. When 0.46<R_S<1, 1.01<R_K<1.023. Then, interference effects start to appear in double collinear cracks tips, but the degree of interference is little. When 0<R_S<0.46, R_K>1.023. Then, interference effects between the double collinear cracks become severe and the strengthening effect becomes remarkable.

The fatigue lives of double collinear cracks before

the coalescence in the cases of the initial horizontal crack spacing $S=8c_0$, $14c_0$, $18c_0$, $24c_0$ are plotted in Fig. 4. When $S=8c_0$, R_S changes from 4 to 0.46, and load cycle number N=492784; when $S=14c_0$, R_S changes from 7.5 to 0.46, and N=686564; when $S=18c_0$, R_S changes from 9 to 0.46, and N=770074; when $S=24c_0$, R_S changes from 12 to 0.46, and N=843227.

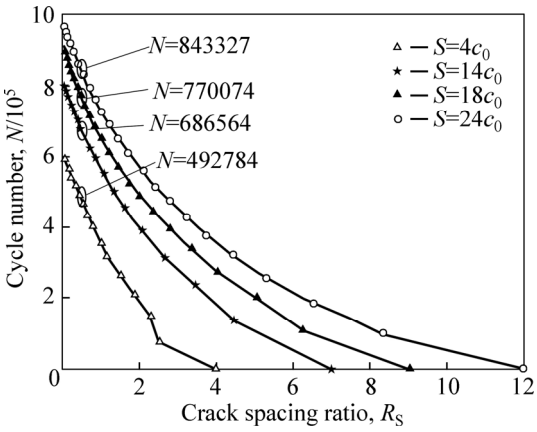

Fig. 4 Load cycle number of double collinear cracks before process of coalescence

The design life of the Three Gorges shiplift is 70 years, working 335 days per year and operating 18 times (each time contains a rise and a fall) per day on average. Load cycle number is equal to 844200. If R_S does not reach 0.46 within the design life of shiplift, it is convinced that there are no interference effects between double collinear cracks in the process of propagation. Therefore, in the case that initial crack sizes a_0=3 mm and $2c_0$=6 mm, and horizontal spacing, S, reaches $24c_0$, R_S is greater than 0.46 (within the design life of shiplift), and the two cracks are regarded to be isolated. Accordingly, the horizontal crack spacing threshold, S_C, for the double collinear cracks is $24c_0$.

3.2 Crack propagation during process of coalescence

When the horizontal spacing of the double collinear cracks decreases to zero, the inner crack tips B and C contact each other and double cracks enter the coalescence period. Figure 5(a) shows the crack length variation rule of double collinear cracks which propagates from initial state to the completion of coalescence in the cases of $S=2c_0$, $8c_0$, $14c_0$, respectively. Immediately after the coalescence of double collinear cracks, there is a sharp increase in crack length. And then, the growth rate in length direction decreases until the end of the coalescence.

On the other hand, the depth direction of the new single crack in central area increases sharply (Fig. 5(b)). After the cracks coalesce completely, the growth rates in length direction and depth direction are consistent with those of semi-elliptical single crack in the two directions.

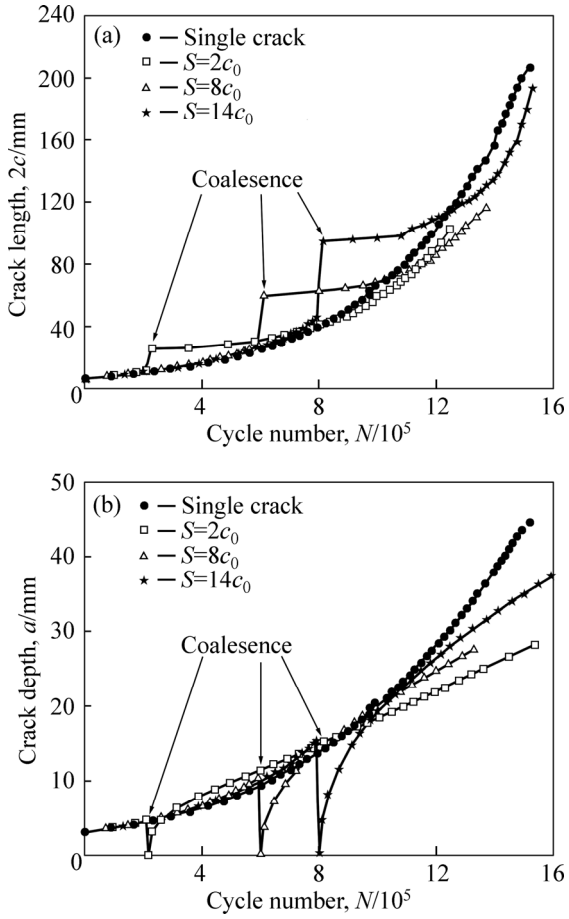

Fig. 5 Variation rule of crack length and crack depth during process of coalescence of double collinear cracks under various horizontal spacings: (a) Crack length; (b) Crack depth

Therefore, the average growth rate of crack center depth, during the coalescing process, is defined as V_1, and the average growth rate of coalesced crack is defined as V_2. The maximum value reaches $V_1=7.57\times10^{-5}$ mm/cycle when $S=14c_0$, and $V_1/V_2=2.64$. The average growth rate of crack center depth is given in Table 1.

Table 1 Average growth rate of crack center depth under various horizontal spacings

S	V_1/(mm·cycle^{-1})	V_2/(mm·cycle^{-1})	V_1/V_2
$2c_0$	3.81×10^{-5}	1.79×10^{-5}	2.13
$8c_0$	5.88×10^{-5}	5.88×10^{-5}	2.39
$14c_0$	7.57×10^{-5}	2.86×10^{-5}	2.64

4 Vertical spacing threshold of double parallel offset cracks

In order to describe the interference effects on double parallel offset cracks of the large-module rack, and further, to explore the vertical crack spacing threshold, double semi-elliptical offset cracks in the same size are inserted in the sub-model. The initial crack

depth a_0=3 mm, length $2c_0$=6 mm and horizontal spacing $S=2c_0$. Tips *A* (top crack) and *D* (bottom crack) represent the outer crack tips. Tips *B* (top crack) and *C* (bottom crack) represent the inner crack tips. The vertical spacing, *h*, is set to be c_0, $2c_0$, $3c_0$ and $4c_0$. The parameter *E* represents the distance of outer crack tips (Fig. 6) and it is regarded as the size evidence to judge whether offset cracks interfere or not.

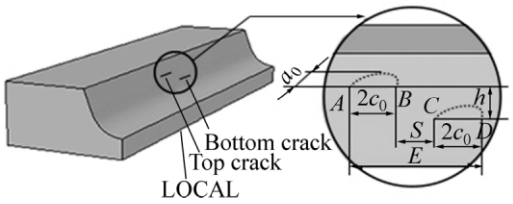

Fig. 6 Simulation model of double parallel offset cracks

Double parallel offset cracks of the large-module rack are different from those of semi-infinite, of which the loads on top and bottom are different. Therefore, whether interference effects have influence on double parallel offset cracks of the large-module rack can not be judged through the comparison with the SIF of single crack tip, K_{I_single}. It is necessary to build the double offset cracks models with no interference effects which suit for the large-module rack.

The single bottom crack and the single top crack with $h=c_0$, $2c_0$, $3c_0$, $4c_0$, respectively, are inserted in two rack sub-models (Fig. 7). The crack tip SIF of the double offset cracks and that in condition of no interference effect models are calculated under the same load cycle number, *N*, respectively.

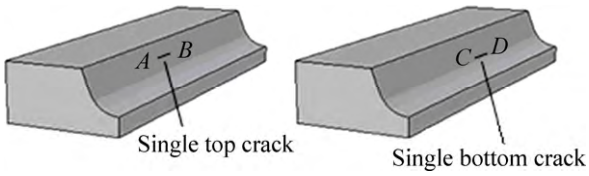

Fig. 7 Simulation model of double cracks with no interference effect

(1) $h=c_0$

The horizontal spacing, *S*, of the inner crack tips decreases gradually in the propagation process of the double parallel offset cracks. *S* value becoming negative represents the overlap of cracks. After comparing with the crack model with no interference effects, it can be found that the inner crack tip of the bottom crack is affected by strengthening effect before *S* decreases to −1.1 mm, and then, it is affected by inhibiting effect due to crack tip shielding effect (Fig. 8(a)). The top crack is affected by strengthening effect before *S* decreases to

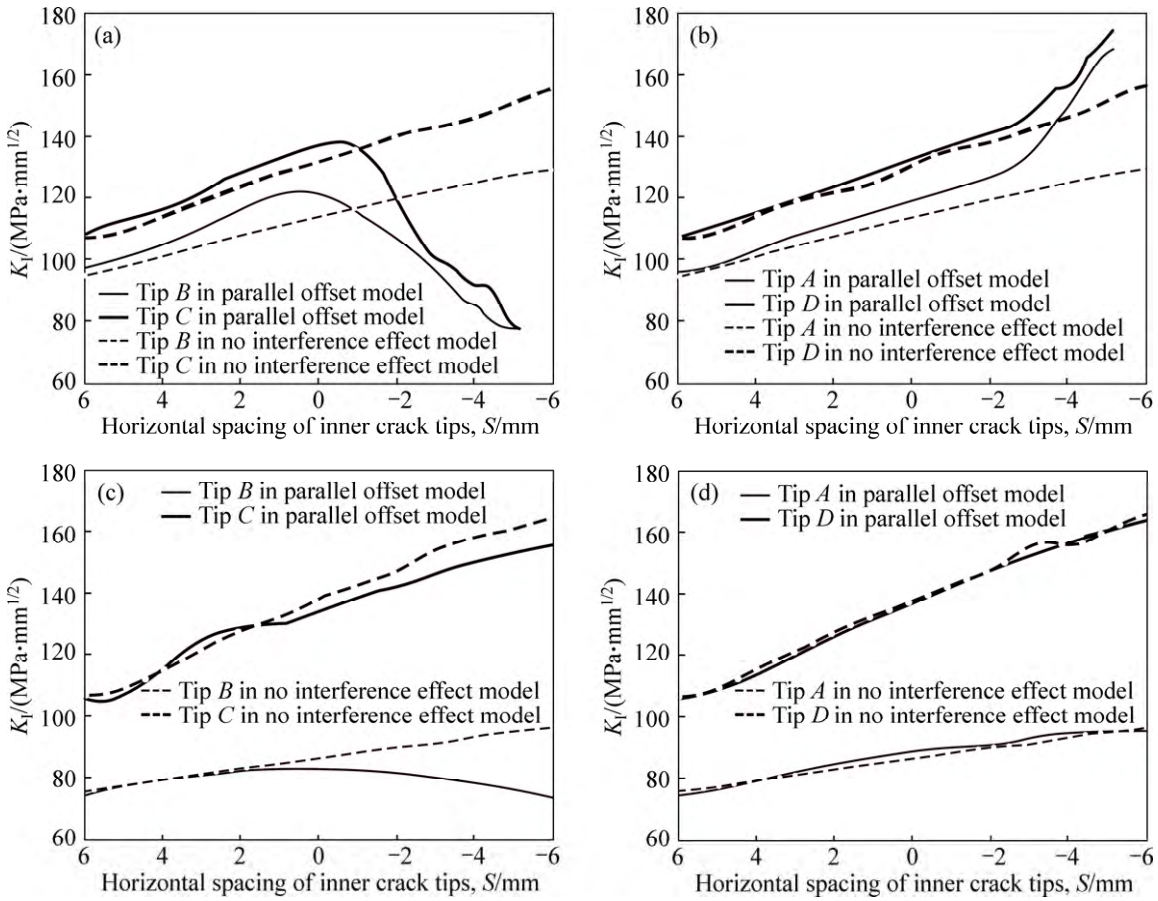

Fig. 8 Comparison of crack tip stress intensity factor with double parallel offset cracks and no interference effects double cracks at $h=c_0$ and $4c_0$: (a) $h=c_0$, inner crack tips; (b) $h=c_0$, outer crack tips; (c) $h=4c_0$, inner crack tips; (d) $h=4c_0$, outer crack tips

−0.8 mm. After S reduces to −0.8 mm, it is affected by inhibiting effect. According to the findings, it can also be found that the top crack enters into the inhibiting effect zone earlier than the bottom crack. However, the outer crack tips always locate in the strengthening effect zone, and the influence is obvious after S decreases to −2.5 mm (Fig. 8(b)).

(2) $h=4c_0$

The inner crack tip of the bottom crack is affected by strengthening effect before S decreases to 2 mm. After that, it is affected by inhibiting effect. However, the inner crack tip of the top crack is affected by inhibiting effect (Fig. 8(c)) all the time. In terms of double parallel offset crack model and crack model with no interference effects, their curves of outer crack tip SIF roughly coincide. Therefore, it can be thought of no interference effects between double parallel offset cracks (Fig. 8(d)).

With the same load cycle number, the distance of outer crack tips, E, is calculated in the cases of double offset cracks and double cracks with no interference effects, respectively. The vertical spacing, h, ranges from c_0 to $4c_0$.

When h ranges from c_0 to $3c_0$, the E value in the case of double offset cracks is greater than that in the case of no interference effects during the propagation process, which reveals that when h ranges from c_0 to $3c_0$, strengthening effect has influence on the crack propagation. According to regional analysis of crack propagation interference effects, the inner crack tips in the initiative strengthening zone enter into the inhibition zone gradually, and the outer crack tips are always in a strengthening effect zone. In general, there is strengthening effect on the crack propagation comprehensively (Figs. 9(a)−(b)).

When h reaches $4c_0$, in terms of double offset cracks model and crack model with no interference effects, their curves of the E value roughly coincide (Fig. 8(b)), which reveals that double offset cracks propagation has no obvious influence on the whole crack propagation. These findings match the analysis of stress intensity factor (Fig. 8). As a consequence, when the vertical spacing of parallel offset cracks is equal or greater than $4c_0$, the double cracks are regarded to be isolated. Therefore, the vertical crack spacing threshold h_C for the parallel offset double cracks is $4c_0$.

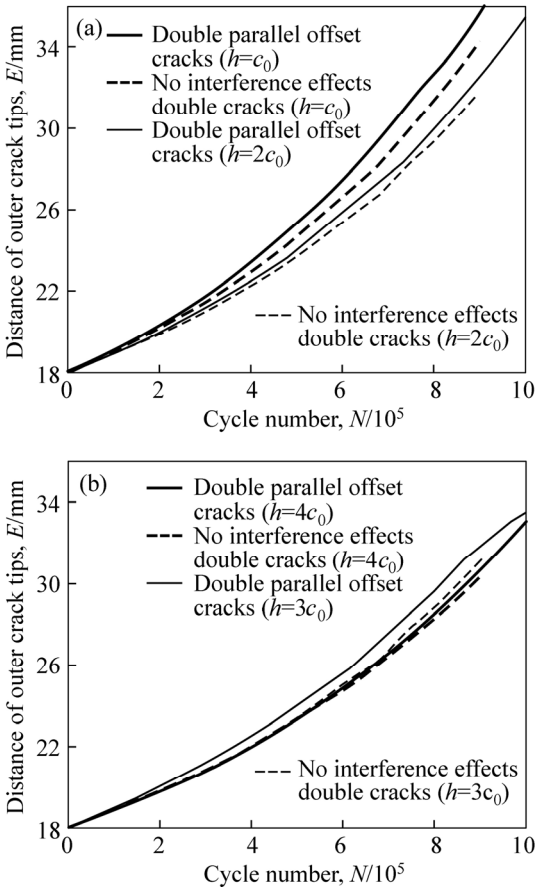

Fig. 9 Comparison of distance of outer crack tips with double parallel offset cracks and no interference effects double cracks: (a) $h=c_0$ and $2c_0$; (b) $h=3c_0$ and $4c_0$

5 Conclusions

1) The variation rule of influence factors of SIF, R_K, changing with horizontal spacing ratio, R_S, of the double collinear cracks is obtained. If $0<R_S<0.46$, then $R_K>1.023$ and interference effects between the double collinear cracks become obvious. If $0.46<R_S<1$, then $1.01<R_K<1.023$ and interference effects appear between double collinear cracks. However, its strengthening effect is not significant. If $R_S>1$, then $R_K<1.01$, and there is nearly no interference effects between double collinear cracks in the propagation process, thus they are regarded as two isolated cracks.

2) When the vertical spacing, h, of parallel offset cracks ranges from c_0 to $3c_0$, the inner crack tips enter into the inhibiting effect area from the strengthening effect area gradually. Distance of the outer crack tips, E, is greater than that of double cracks with no interference effects, if the load cycle number, N, is the same. When $h\geq 4c_0$, the E value equals that of the double cracks with no interference effects, which means that the interference effects on double offset cracks have no apparent effects on the whole crack size.

3) Immediately after coalescence of double collinear cracks, there is a sharp increase in crack length, and there is a dramatic increase of crack center depth during coalescing. The average growth rate of crack center depth can reach 7.57×10^{-5} mm/cycle at most, which is 2.64 times as fast as the center depth growth rate of coalesced cracks.

4) In the case that the initial crack sizes a_0=3 mm and $2c_0$=6 mm, within 70 years of the design life of the

shiplift, if $S \geq 24c_0$, then R_S will not reach 0.46 and two cracks can be regarded to be isolated. The horizontal crack spacing threshold of the double collinear cracks $S=24c_0$. When the vertical spacing of parallel offset cracks is equal to or greater than $4c_0$, the double cracks are regarded to be isolated. Therefore, in terms of the parallel offset double cracks, the vertical crack spacing threshold $h=4c_0$.

References

[1] SPIEVAK L E, WAWRZYNEK P A, INGRAFFEA A R, LEWICKI D G. Simulating fatigue crack growth in spiral bevel gears [J]. Engineering Fracture Mechanics, 2001, 68(1): 53−76.

[2] URAL A, HEBER G, WAWRZYNEK P A, INGRAFFEA A R, LEWICKI D G, NETO J B C. Three-dimensional, parallel, finite element simulation of fatigue crack growth in a spiral bevel pinion gear [J]. Engineering Fracture Mechanics, 2005, 72: 1148−1170.

[3] SHAO Ren-ping, JIA Pu-rong, DONG Fei-fei. Dynamic characteristics of cracked gear and three-dimensional crack propagation analysis [J]. Mechanical Engineering Science, 2013, 227: 1341−1361.

[4] SAMROENG N, PANYA S. Failure of a helical gear in a power plant [J]. Engineering Failure Analysis, 2013, 32: 81−90.

[5] ANDREA C, ROBERTO B, SABRINA V. A numerical analysis on the interaction of twin coplanar flaws [J]. Engineering Fracture Mechanics, 2004, 71: 485−499.

[6] HUANG Yi, CHEN Jing-jie, LIU Gang. Research on calculation of SIF for multi collinear cracks based on maximum crack opening displacement [J]. Mechanical Strength, 2010(6): 1002−1007. (in Chinese)

[7] WANG Bing, ZHANG Xiu-fang, DAI Jian-guo, XU Shi-lang. Critical crack tip opening displacement of different strength concrete [J]. Journal of Central South University, 2011, 18: 1693−1699.

[8] MASAYUKI K. Growth evaluation of multiple interacting surface cracks. Part I: Experiments and simulation of coalesced crack [J]. Engineering Fracture Mechanics, 2008, 75: 1336−1349.

[9] MASAYUKI K. Growth evaluation of multiple interacting surface cracks. Part II: Experiments and simulation of coalesced crack [J]. Engineering Fracture Mechanics, 2008, 75: 1350−1366.

[10] MASAYUKI K, NOBUO T. Influence of interaction between multiple cracks on stress corrosion crack propagation [J]. Science, 2002, 44: 2333−2352.

[11] KIKUCHI M, WADA Y, SUGA K, OHDAMA C. Numerical simulation of coalescence behavior of multiple surface cracks [C]// ASME 2011 Pressure Vessels and Piping Conference. 2011, 441−446.

[12] TAN J T, CHEN B K. Coalescence and growth of two coplanar short cracks in AA7050-T7451 aluminium alloys [J]. Engineering Fracture Mechanics, 2013, 102: 324−333.

[13] MA Jie, SHAO Ren-ping, DONG Fei-fei. Three dimensional extended analysis and life prediction of gear crack [J]. Applied Mechanics and Materials, 2012, 121/122/123/124/125/126: 4863−4869.

[14] YU Guo-peng, DUAN Qing-quan, ZHANG Hong. The fatigue constant of paris formula gained by finite element method [J]. Welded Pipe and Tube, 2009(6): 18−20, 25. (in Chinese)

[15] LI Qing-fen. Fracture mechanics and engineering application [M]. Harbin: Harbin Shipbuilding Institute Press, 1998: 135−136. (in Chinese)

(Edited by YANG Bing)